

From Microscales to Macroscales in 3D: Selfconsistent Equation of State for Supernova and Neutron Star Models

W G Newton¹, J R Stone^{1,2,3}, A Mezzacappa²

¹ Department of Physics, University of Oxford, Oxford OX1 3PU, United Kingdom

² Physics Division, Oak Ridge National Laboratory, P.O. Box 2008, Oak Ridge, TN 37831, USA

³ Department of Chemistry and Biochemistry, University of Maryland, College Park, MD 20742, USA

E-mail: william.newton@seh.ox.ac.uk, stonejr@ornl.gov, mezzacappaa@ornl.gov

Abstract. First results from a fully self-consistent, temperature-dependent equation of state that spans the whole density range of neutron stars and supernova cores are presented. The equation of state (EoS) is calculated using a mean-field Hartree-Fock method in three dimensions (3D). The nuclear interaction is represented by the phenomenological Skyrme model in this work, but the EoS can be obtained in our framework for any suitable form of the nucleon-nucleon effective interaction. The scheme we employ naturally allows effects such as (i) neutron drip, which results in an external neutron gas, (ii) the variety of exotic nuclear shapes expected for extremely neutron heavy nuclei, and (iii) the subsequent dissolution of these nuclei into nuclear matter. In this way, the equation of state is calculated across phase transitions without recourse to interpolation techniques between density regimes described by different physical models. EoS tables are calculated in the wide range of densities, temperature and proton/neutron ratios on the ORNL NCCS XT3, using up to 2000 processors simultaneously.

1. Introduction

Observational properties of neutron stars and supernovae serve as powerful constraints of the nuclear EoS. There is a large variety of EoS models in the literature and it is imperative to investigate the connection of the physical processes expected in stars with the features of individual EoS. The models used to construct nuclear EoS range from empirical to those based on non-relativistic effective and realistic nucleon-nucleon potentials and relativistic field theories (for a recent reviews see e.g. [1, 2]). It is unclear at present which of these EoS is closest to reality. All the EoS are required to reflect physics occurring in a wide region of particle number densities. In core-collapse supernovae these densities span from the subnuclear density of about 4×10^{-8} to $\sim 0.1 \text{ fm}^{-3}$ (inhomogeneous matter) to the high density phase (uniform matter) between $\sim 0.1 \text{ fm}^{-3} - 0.6 \text{ fm}^{-3}$. Neutron star models involve an even wider density range starting from $\sim 6 \times 10^{-15} \text{ fm}^{-3}$ (estimated density at the surface of neutron stars) to about $0.6 - 1.0 \text{ fm}^{-3}$ (expected in the center of neutron stars). Most of the currently used EoSs in both the subnuclear and supernuclear density do not cover the whole range but are composed of several EoSs reflecting the evolution of the character of matter with changing density in smaller intervals. One of the most interesting density regions covers the transition between

uniform and inhomogeneous matter, known as the ‘pasta’ phase. In this region superheavy neutron rich nuclei beyond the neutron drip line gradually dissolve into nucleon + lepton matter of uniform density. The proton and neutron density distribution is determined by a delicate balance between the surface tension of nuclei and the Coulomb repulsion of protons. Previous models of the ‘pasta’ phase of matter, assuming spherical symmetry, predicted the existence of a series of exotic nuclear shapes - rods, slabs, tubes and bubbles, immersed in a free neutron and electron gas, corresponding to minimal energy of the matter as a function of increasing density, until the uniform distribution becomes energetically favorable. The ‘pasta’ phase of stellar matter, although occurring in a relatively small region of density, has a significant influence on the neighboring higher and lower density regions due to the requirement of continuity and thermodynamical consistency of the energy per particle and related quantities throughout the whole density and temperature range.

The focus of this work is on the EoS that serves as an input to core-collapse supernova models and non-equilibrium young neutron stars. However, only a slight modification, i.e. the inclusion of chemical equilibrium at supernuclear densities, is required to use this EoS in old neutron stars. The most widely used EoS in core-collapse supernova simulations so far have been the non-relativistic EoS by Lattimer-Swesty [3] and relativistic mean-field model by Shen et al [4]. Both these EoS describe hot stellar matter assuming spherical symmetry and use different models for matter in different density and temperature regions. It is the aim of this work to show that a fully self-consistent non-relativistic EoS in the Hartree-Fock (HF) approximation [5, 6] in three dimensions (removing the constraint of spherical symmetry) can be constructed in the whole density and temperature region of interest. In this way the matter is treated as an ensemble of nucleons that naturally configure to a distribution corresponding to the minimal energy per particle at given density and temperature. The computation method adopted here is an extension of previous work of Bonche and Vautherin [7] and Hillebrant and Wolff [8] who calculated self-consistent HF EoS at finite temperature but only in the spherically symmetrical case and Magierski and Heenen [9] who developed an HF EoS for the general case of three dimensions but considered only zero temperature.

2. Computational Procedure

Equation of State, determining the pressure of a system as a function of density and temperature, is constructed for stellar matter at the densities and temperatures found during core collapse of a massive star pre- and post-bounce. Such matter is composed primarily of neutrons, protons and electrons, with a significant flux of photons, positrons and neutrinos also present during core collapse. There are three main bulk parameters of the matter, baryon number density n_b , temperature T and proton fraction y_p defined as the ratio of the proton number density n_p to the total baryon number density n_b . In the present work, the ranges of these parameters are $0.001 < n_b < 0.16 fm^{-3}$, $0 < T < 10 MeV$, and $0 < y_p < 0.5$. Furthermore, the EoS is dependent on a number of microscopic parameters, determining the strong force, acting between nucleons in the matter. The phenomenological Skyrme SkM* force [10] is used here but it is easy to modify the computer code for any other applicable model of the nucleon-nucleon interaction. Finally, the electric Coulomb force acting between charged particles, protons and electrons is included. Electrons are treated as forming a degenerate Fermi gas which should be a valid approximation. Neutrinos are not considered at the present stage of the model.

The fundamental assumption used here is that nuclear matter has a periodic character and can be modeled as an infinite sequence of cubic unit cells. This notion removes a serious limitation of all previous models based on consideration of spherical cells which allows only spherically symmetrical nucleon distribution in the cell and cannot fully express the periodic character of matter as the cells make contact only at limited number of points leaving the space between them unaccounted for. Each unit cell contains a certain number of neutrons N and protons

Z , making a total baryon number of $A = N + Z$. Quantum mechanical determination of all energy states and corresponding wave functions of a system of A nucleons in the cell requires exact solution of the A -dimensional equation of motion - the Schroedinger Equation - which is not technically feasible at present. However, if it is assumed that there exists an average single-particle potential, created by all nucleons, in which each nucleon moves independently of all the other nucleons present, then it is possible to use the Hartree-Fock approximation to the A -dimensional problem which reduces it to A one-dimensional problems. A spectrum of discrete energy states, the single-particle states, can be defined in the cell which the individual nucleons occupy (in analogy to a spectrum of standing waves in a box in classical physics). The single-particle wave functions ψ_i , associated with these states, are used to construct the total wavefunction Ψ and to calculate the expectation value of total energy in the state Ψ . Obviously there are many ways the nucleons can be distributed over the available single-particle states, which always considerably outnumber, by a factor of two at least, the total number of nucleons in the cell. Each of these nucleon configurations corresponds to an energy state and a particular spacial distribution of nucleon density in the cell. It turns out that it is possible to find a state Ψ_{\min} , constructed of a set of single-particle states, of which the lowest A states are occupied, which corresponds to the minimum energy of the system and is the best approximation to the true A -particle ground state.

Starting from a trial set of single-particle wave functions ψ_i , the expectation value of total energy is minimized using the variational principle

$$\delta E[\Psi] = 0 \tag{1}$$

This conditions leads to a system of A non-linear equations for ψ_i that has to be solved iteratively. In this work, three forms of the trial wavefunction have been tested, Gaussian times polynomial functions, harmonic oscillator wave functions and plane waves. At the beginning the lowest A trial single-particle states are occupied. After each iteration, the resulting states are reordered according to increasing energy and re-occupied. This approach ensures that the final solution is fully independent from the initial choice of trial wavefunction and it is not predetermined by this choice. The evolution of the shape of neutron density distribution during the iteration process is illustrated for $A=900$ and $y_p=0.3$; in Figs. 1–2 the 3D density distribution is displayed for $n_b=0.08 \text{ fm}^{-3}$, $T=2.5 \text{ MeV}$ and Figs. 3–4 for $n_b=0.12 \text{ fm}^{-3}$, $T=5.0 \text{ MeV}$. The change in the distribution after 500 and several thousand iterations is quite striking. We note that in these figures increase in density is color-coded from blue to red.

Two iteration schemes have been employed to avoid instabilities in the iteration process - the Imaginary Time Step (ITS) and the Damped Gradient Step (DGS). The ITS is very robust and leads to initial rather rapid convergence even when the iteration process is started from trial functions not too similar to the true single-particle wavefunctions. However, when the minimum is approached, it slows down exponentially. The DGS method requires fairly good initial wavefunctions but converges much faster and leads to close to linear convergence for final iterations. In the present work both schemes have been used starting with the ITS and switching over after first few hundred iterations to DGS. After convergence is reached, the total energy density, entropy and pressure and other related observables are calculated and the EoS constructed in tabular form.

It is important to realise that it is not known *a priori* what is the number of particles in the cell at given density that corresponds to the physical size of the unit cell in nature. For each particle number density the volume of a cell is defined as A/n_b and the energy density and the spatial particle density distribution varies significantly with A , as demonstrated in Figs. 5–8 for $n_b=0.08 \text{ fm}^{-3}$, $T=2.5 \text{ MeV}$ and $y_p=0.3$. Each of these results are examples of possible *excited* states of the true unit cell (although they are local ground-states for a given set of parameters). These states are rather close in energy and a series of careful calculations has to be performed

to search for the value of A which gives the absolute minimum energy density for a given set of bulk parameters (i.e. *minimum minimorum*).

3. Results and discussion

One of the main results of the current work is the development of properties of nuclear matter through extended density and temperature regions. At the lower density limit ($n_b < 0.0001 \text{ fm}^{-3}$), the nucleons are arranged as a roughly spherical (but very large) ‘nucleus’ at the centre of the cell. As the density increases, however, the shape deforms and the nucleon density distribution starts to spread out toward the cell boundaries, assuming a variety of exotic forms made of high and low density regions. At the extreme density, the nucleon density distribution becomes uniform. This behaviour is illustrated in Figs. 9–11 which shows neutron density distribution at three selected densities, $T=5 \text{ MeV}$ and $y_p=0.3$ and clearly demonstrates the transition between spherical and homogeneous density distribution.

The entire nucleon configuration within each cell is treated self-consistently as one entity for each set of the macroscopic parameters and evolves naturally within the model as the macroscopic parameters are varied. This is in sharp contrast with previous models where neutron heavy nuclei at and beyond the particle drip-line were considered as immersed in a sea of unbound free nucleons and the two systems were treated separately. In this approach the transition between the inhomogeneous and homogeneous phase of nuclear matter did not emerge naturally from the calculation but had to be imposed artificially, introducing uncertainty about the threshold density region. Furthermore, important phenomena discussed in more detail elsewhere [11] such as shell effects, influence of the lattice structure on Coulomb energy and scattering of weakly bound nucleons on inhomogeneities in the matter are automatically included.

4. Summary

The present model provides the first fully self-consistent 3D picture of hot dense nuclear matter. It offers a new concept of hot nuclear matter in the inner crust of neutron stars and in the transitional density region between non-uniform and uniform matter in collapsing stars. Instead of the traditional notion of super-neutron-heavy nuclei immersed in a free neutron gas it predicts a continuous medium with varying spatial concentration of neutrons and protons. The properties of this medium come out self-consistently from the model, as well as the transitions to both higher and lower density phases of the matter. These results may have profound consequences for macroscopic modelling of core-collapse supernovae and neutron stars. In particular, weak interaction processes (neutrino transport and beta-decay) in such a medium, will have to be investigated.

Acknowledgments

Special thanks go to R. J. Toede, Chao Li Wang, Amy Bonsor and Jonathan Edge for development and performing data visualisation. This work was conducted under the auspices of the TeraScale Supernova Initiative, funded by SciDAC grants from the DOE Office of Science High-Energy, Nuclear, and Advanced Scientific Computing Research Programs and partly supported by US DOE grant DE-FG02-94ER40834. Resources of the Center for Computational Sciences at Oak Ridge National Laboratory were used. Oak Ridge National Laboratory is managed by UT-Battelle, LLC, for the U.S. Department of Energy under contract DE-AC05-00OR22725.

References

- [1] Lattimer J. M and Prakash M 2000 *Phys. Rep.* **334** 121.
- [2] Stone J. R 2006 *Open Issues in Understanding of Core-Collapse Supernova Theory* ed. A Mezzacappa and G M Fuller (World Scientific) p 318
- [3] Lattimer J. M and Swesty F. D 1991 *Nucl.Phys. A* **535** 331
- [4] Shen H, Toki H, Oyamatsu K and Sumiوشي K 1998 *Nucl.Phys. A* **637** 435
- [5] Hartree D R 1928 *Proc.Camb.Phil.Soc.* **24** 89
- [6] Fock V A 1930 *Z.Phys* **61** 126
- [7] Bonche P and Vautherin D 1981 *Nucl.Phys. A* **372** 496
- [8] Hillebrandt W and Wolff R.- G 1985 *Nucleosynthesis:Challenges and New Developments* ed. D Arnett and J W Truran A (Univ. Chicago) p 131
- [9] Magierski P and Heenen P.-H 2002 *Phys. Rev. C* **65** 045804
- [10] Bartel J, Quentin P, Brack M, Guet C, and Hakansson H.-B 1982 *Nucl.Phys. A* **386** 79
- [11] Newton W G, 2006 *DPhil Thesis* Oxford University

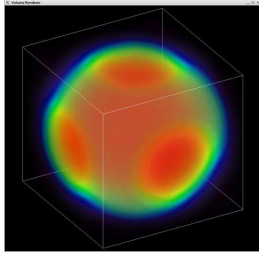


Figure 1. 3D neutron density distribution after 500 iterations.

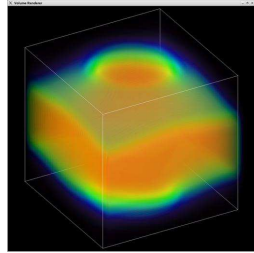


Figure 2. 3D neutron density distribution after 2800 iterations.

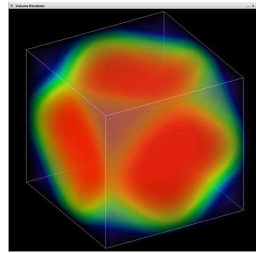


Figure 3. 3D neutron density distribution after 500 iterations.

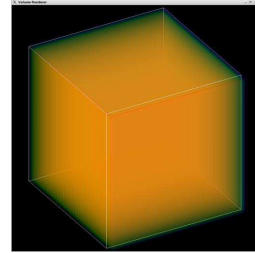


Figure 4. 3D neutron density distribution after 6500 iterations.

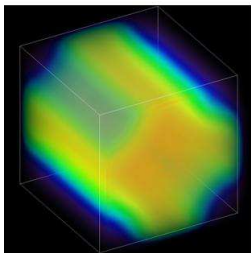


Figure 5. Neutron density distributions for $A=180$.

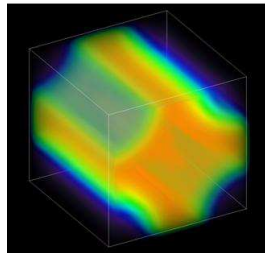


Figure 6. The same as Fig. 5 but for $A=460$.

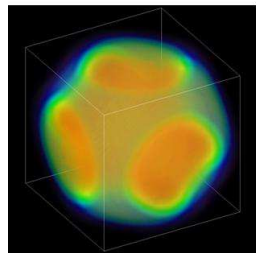


Figure 7. The same as Fig. 5 but for $A=1400$.

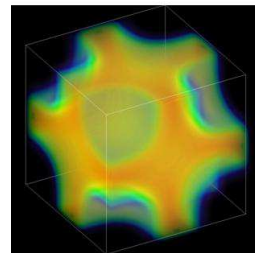


Figure 8. The same as Fig. 5 but for $A=2200$.

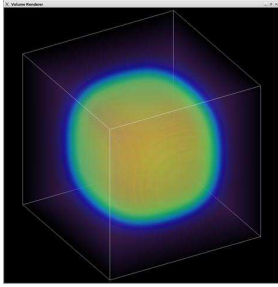


Figure 9. 3D neutron density distribution at $n_b=0.04 \text{ fm}^{-3}$.

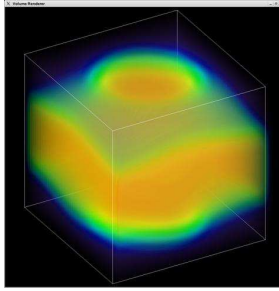


Figure 10. 3D neutron density distribution at $n_b=0.08 \text{ fm}^{-3}$.

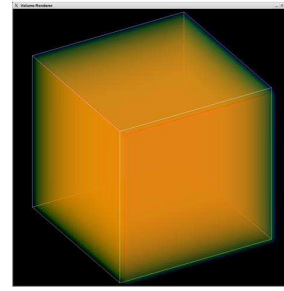


Figure 11. 3D neutron density distribution at $n_b=0.12 \text{ fm}^{-3}$.